Article

Solvation Dynamics in Ni(HO) Clusters Probed with Infrared Spectroscopy

Richard S. Walters, E. Dinesh Pillai, and Michael A. Duncan

J. Am. Chem. Soc., **2005**, 127 (47), 16599-16610• DOI: 10.1021/ja0542587 • Publication Date (Web): 03 November 2005

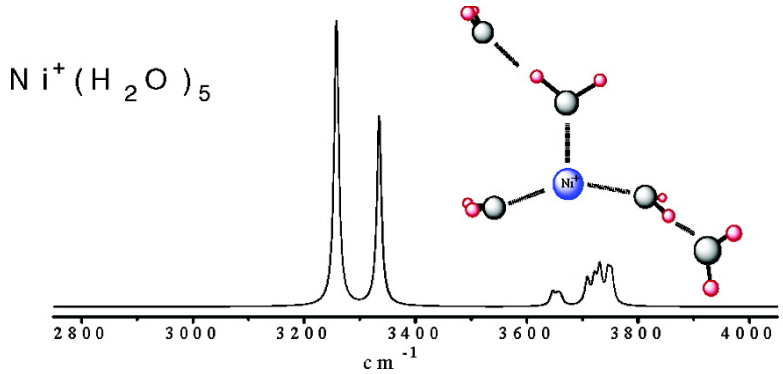

More About This Article

Additional resources and features associated with this article are available within the HTML version:

- Supporting Information
- Links to the 14 articles that cite this article, as of the time of this article download
- Access to high resolution figures
- Links to articles and content related to this article
- Copyright permission to reproduce figures and/or text from this article

View the Full Text HTML

J|A|C|S
ARTICLES
Published on Web 11/03/2005

Solvation Dynamics in $Ni^+(H_2O)_n$ Clusters Probed with Infrared Spectroscopy

Richard S. Walters, E. Dinesh Pillai, and Michael A. Duncan*

Contribution from the Department of Chemistry, University of Georgia, Athens, Georgia 30602-2556

Received June 28, 2005; E-mail: maduncan@uga.edu

Abstract: Infrared photodissociation spectroscopy is reported for mass-selected $Ni^+(H_2O)_n$ complexes in the O−H stretching region up to cluster sizes of $n = 25$. These clusters fragment by the loss of one or more intact water molecules, and their excitation spectra show distinct bands in the region of the symmetric and asymmetric stretches of water. The first evidence for hydrogen bonding, indicated by a broad band strongly red-shifted from the free OH region, appears at the cluster size of $n = 4$. At larger cluster sizes, additional red-shifted structure evolves over a broader wavelength range in the hydrogen-bonding region. In the free OH region, the symmetric stretch gradually diminishes in intensity, while the asymmetric stretch develops into a closely spaced doublet near 3700 cm^{-1}. The data indicate that essentially all of the water molecules are in a hydrogen-bonded network by the size of $n = 10$. However, there is no evidence for the formation of clathrate structures seen recently via IR spectroscopy of protonated water clusters.

Introduction

The solvation of metal cations by water is ubiquitous throughout chemistry and biology.[1−3] However, the energetics and dynamics of this process result from the subtle interplay of electrostatic and covalent interactions that are challenging to understand at the molecular level. Gas-phase metal ion complexes provide convenient models for cation solvation processes and for studies of so-called "aqua ions" in isolated form.[4−6] Although the degree of correspondence between such gas-phase systems and solvation in the condensed phase is not yet clear, metal ion complexes provide finite-sized systems that can be investigated in detail with both experiment and theory. Various mass spectrometry methods have been employed to study such complexes,[7−19] and theory has investigated their structures and energetics.[20−29] However, spectroscopic probes of solvation in metal ion complexes have been limited.[30−39] In recent years, advances in infrared photodissociation spectroscopy are beginning to shed light on the structures and growth dynamics of metal ion complexes as a function of size.[37−49] In the present study, we report IR spectroscopy for $Ni^+(H_2O)_n$ complexes in the OH stretching region. Spectroscopy over the size range of $n = 1−25$ investigates the nascent solvation process.

Metal cation complexes with water have been produced and studied in mass spectrometry for many years. Equilibrium

(1) Hunt, J. P. *Metal Ions in Aqueous Solution*; W. A. Benjamin and Sons: New York, 1963.
(2) (a) Burgess, J. *Metal Ions in Solution*; John Wiley and Sons: New York, 1978. (b) Burgess, J. *Ions in Solution*; Horwood Publishing: Chichester, U.K., 1999.
(3) Richens, D. T. *The Chemistry of Aqua Ions*; John Wiley: Chichester, U.K., 1997.
(4) Freiser, B. S.; Ed. *Organometallic Ion Chemistry*; Kluwer: Dordrecht, The Netherlands, 1996.
(5) Duncan, M. A.; Ed. *Advances in Metal and Semiconductor Clusters*; Elsevier: Amsterdam, 2001; Vol. 5.
(6) Duncan, M. A. *Int. J. Mass Spectrom.* **2000**, *200*, 545.
(7) Kebarle, P. *Annu. Rev. Phys. Chem.* **1977**, *28*, 445.
(8) Marinelli, P. J.; Squires, R. R. *J. Am. Chem. Soc.* **1989**, *111*, 4101.
(9) (a) Magnera, T. M.; David, D. E.; Michl, J. *J. Am. Chem. Soc.* **1989**, *111*, 4100. (b) Magnera, T. M.; David, D. E.; Stulik, D.; Orth, R. G.; Jonkman, H. T.; Michl, J. *J. Am. Chem. Soc.* **1989**, *111*, 5036.
(10) (a) Dalleska, N. F.; Honma, K.; Sunderlin, L. S.; Armentrout, P. B. *J. Am. Chem. Soc.* **1994**, *116*, 3519. (b) Clemmer, D. E.; Chen, Y.-M.; Aristov, N.; Armentrout, P. B. *J. Phys. Chem.* **1994**, *98*, 7538. (c) Dalleska, N. F.; Tjelta, B. L.; Armentrout, P. B. *J. Phys. Chem.* **1994**, *98*, 4191. (d) Rogers, M. T.; Armentrout, P. B. *J. Phys. Chem. A* **1997**, *101*, 1238. (e) Koizumi, H.; Larson, M.; Muntean, F.; Armentrout, P. B. *Int. J. Mass Spectrom.* **2003**, *228*, 221.
(11) (a) Poisson, L.; Lepetit, F.; Mestdagh, J.-M.; Visticot, J.-P. *J. Phys. Chem. A* **2002**, *106*, 5455. (b) Poisson, L.; Dukan, L.; Sunlemontier, O.; Lepetit, F.; Reau, F.; Pradel, P.; Mestdagh, J.-M.; Visticot, J.-P. *Int. J. Mass Spectrom.* **2002**, *220*, 111. (c) Poisson, L.; Pradel, P.; Lepetit, F.; Reau, F.; Mestdagh, J.-M.; Visticot, J.-P. *Eur. Phys. J. D* **2001**, *14*, 89. (d) Dukan, L.; del Fabbro, L.; Pradel, P.; Sunlemontier, O.; Mestdagh, J.-M.; Visticot, J.-P. *Eur. Phys. J. D* **1998**, *3*, 257.
(12) Harms, A. C.; Khanna, S. N.; Chen, B.; Castleman, A. W., Jr. *J. Chem. Phys.* **1994**, *100*, 3540.
(13) (a) Beyer, M. B. C.; Gorlitzer, H. W.; Schindler, T.; Achatz, U.; Albert, G.; Niedner-Schatteburg, G.; Bondybey, V. E. *J. Am. Chem. Soc.* **1996**, *118*, 7386. (b) Beyer, M. A.; Achatz, U.; Berg, C.; Joos, S.; Niedner-Schatteburg, G.; Bondybey, V. E. *J. Phys. Chem. A* **1999**, *103*, 671. (c) Bondybey, V. E.; Beyer, M. K. *Int. Rev. Phys. Chem.* **2002**, *21*, 277. (d) Fox, B. S.; Balteanu, I.; Balaj, O. P.; Liu, H.; Beyer, M. K.; Bondybey, V. E. *Phys. Chem. Chem. Phys.* **2002**, *4*, 2224. (e) Berg, C.; Achatz, U.; Beyer, M. K.; Joos, S.; Albert, G.; Schindler, T.; Niedner-Schatteburg, G.; Bondybey, V. E. *Int. J. Mass Spectrom.* **1997**, *167/168*, 723. (f) Berg, C.; Beyer, M. K.; Achatz, U.; Joos, S.; Niedner-Schatteburg, G.; Bondybey, V. E. *Chem. Phys.* **1998**, *239*, 379. (g) Bondybey, V. E.; Beyer, M. K.; Achatz, U.; Fox, B.; Niedner-Schatteburg, G. *Adv. Met. Semicond. Clusters* **2001**, *5*, 295.
(14) (a) Klassen, J. S.; Ho, Y.; Blades, A. T.; Kebarle, P. *Adv. Gas-Phase Ion Chem.* **1998**, *3*, 255. (b) Peschke, M.; Blades, A. T.; Kebarle, P. *J. Phys. Chem. A* **1998**, *102*, 9978. (c) Nielsen, S. B.; Masella, M.; Kebarle, P. *J. Phys. Chem. A* **1999**, *103*, 9891. (d) Peschke, M.; Blades, A. T.; Kebarle, P. *Int. J. Mass Spectrom.* **1999**, *185/186/187*, 685. (e) Peschke, M.; Blades, A. T.; Kebarle, P. *J. Am. Chem. Soc.* **2000**, *122*, 10440. (f) Peschke, M.; Blades, A. T.; Kebarle, P. *Adv. Met. Semicond. Clusters* **2001**, *5*, 77.
(15) (a) Stace, A. J.; Walker, N. R.; Firth, S. *J. Am. Chem. Soc.* **1997**, *119*, 10239. (b) Walker, N. R.; Firth, S.; Stace, A. J. *Chem. Phys. Lett.* **1998**, *292*, 125. (c) Walker, N.; Dobson, M. P.; Wright, R. R.; Barran, P. E.; Murrell, J. N.; Stace, A. J. *J. Am. Chem. Soc.* **2000**, *122*, 11138. (d) Stace, A. J. *Adv. Met. Semicond. Clusters* **2001**, *5*, 121. (e) Cox, H.; Akibo-Betts, G.; Wright, R. R.; Walker, N. R.; Curtis, S.; Duncombe, B.; Stace, A. J. *J. Am. Chem. Soc.* **2003**, *125*, 233. (f) Stace, A. J. *J. Phys. Chem. A* **2002**, *106*, 7993.

measurements, collision-induced dissociation, and radiative association reactions have been employed to determine metal−water binding energies.[7−19] These studies have investigated singly charged metal ions more extensively because they are easier to form in the gas phase,[7−13] but recent experiments have been extended to multiply charged metal systems.[14−19] Theory has investigated the structures that form when water binds to a metal cation, the distortion of the water molecule that accompanies this binding, and the metal−water dissociation energies.[20−29] Because of the low density of gas-phase ions that can be produced, absorption spectroscopy is not feasible and various forms of so-called "action" spectroscopy have been applied to these systems. Electronic photodissociation spectroscopy has been productive for the singly charged alkaline-earth-metal complexes.[30−32] These species have a single valence electron on the metal that gives rise to strongly allowed metal-based electronic transitions. Transition-metal complexes have been studied through similar electronic spectroscopy based on low-lying excited states corresponding to different configurations of the valence d electrons.[33,34] New ion sources (e.g., electrospray) have produced water complexes with multiply charged metal cations, but the spectroscopy of these species is still in its infancy.[34] ZEKE spectroscopy has been demonstrated for monohydrated metals, providing vibrational information for the ground electronic states of the cations.[35,36] IR photodissociation spectroscopy was first described by Lisy and co-workers for alkali-metal cation complexes with water,[37] but our group[38] and others[39] have now extended this method to small cation−water complexes with higher melting point metals.

IR spectroscopy is particularly informative for studies of ion−water complexes because of the convenience of measurements in the O−H stretching region. The frequencies of the isolated water molecule (3657 and 3756 cm^{-1} for the symmetric and asymmetric stretches)[50] shift in predictable ways upon complexation. In particular, it is well-known that hydrogen bonding causes a strong shift to lower frequencies (3200−3400 cm^{-1}) compared to those of the "free O−H" stretches that are found closer to the frequencies for the isolated water molecule.[51−54]

(16) Schroeder, D.; Schwarz, H.; Wu, J.; Desdemiotis, C. *Chem. Phys. Lett.* **2001**, *343*, 258.
(17) (a) Rodriguez-Cruz, S.; Jockusch, R. A.; Williams, E. R. *J. Am. Chem. Soc.* **1998**, *120*, 5842. (b) Rodriguez-Cruz, S.; Jockusch, R. A.; Williams, E. R. *J. Am. Chem. Soc.* **1999**, *121*, 1986. (c) Rodriguez-Cruz, S.; Jockusch, R. A.; Williams, E. R. *J. Am. Chem. Soc.* **1999**, *121*, 8898. (c) Wong, R. L.; Paech, K.; Williams, E. R. *Int. J. Mass Spectrom.* **2004**, *232*, 59.
(18) Shvartsburg, A. A.; Siu, K. W. M. *J. Am. Chem. Soc.* **2001**, *123*, 10071.
(19) (a) Hrusak, J.; Stoeckigt, D.; Schwarz, H. *Chem. Phys. Lett.* **1994**, *221*, 518. (b) Hrusak, J.; Schroeder, D.; Schwarz, H. *Chem. Phys. Lett.* **1994**, *225*, 416.
(20) (a) Rosi, M.; Bauschlicher, C. W., Jr. *J. Chem. Phys.* **1989**, *90*, 7264. (b) Rosi, M.; Bauschlicher, C. W., Jr. *J. Chem. Phys.* **1990**, *92*, 1876. (c) Bauschlicher, C. W., Jr.; Partridge, H. *J. Phys. Chem.* **1991**, *95*, 3946. (d) Bauschlicher, C. W., Jr.; Langhoff, S. R.; Partridge, H. *J. Chem. Phys.* **1991**, *94*, 2068. (e) Bauschlicher, C. W., Jr.; Sodupe, M.; Partridge, H. *J. Chem. Phys.* **1992**, *96*, 4453. (f) Partridge, H.; Bauschlicher, C. W., Jr. *Chem. Phys. Lett.* **1992**, *195*, 494. (f) Sodupe, M.; Bauschlicher, C. W., Jr. *Chem. Phys. Lett.* **1993**, *212*, 624. (g) Ricca, A.; Bauschlicher, C. W., Jr. *J. Phys. Chem. A* **1995**, *99*, 9003. (h) Ricca, A.; Bauschlicher, C. W., Jr. *J. Phys. Chem. A* **2002**, *106*, 3219.
(21) (a) Watanabe, H.; Iwata, S.; Hashimoto, K.; Misaizu, F.; Fuke, K. *J. Am. Chem. Soc.* **1995**, *117*, 755. (b) Watanabe, H.; Iwata, S. *J. Phys. Chem. A* **1997**, *101*, 487. (c) Watanabe, H.; Iwata, S. *J. Chem. Phys.* **1998**, *108*, 10078. (d) Fuke, K.; Hashimoto, K.; Iwata, S. *Adv. Chem. Phys.* **1999**, *110*, 431. (e) Watanabe, H.; Iwata, S. *J. Phys. Chem.* **1996**, *100*, 3377.
(22) Adamo, C.; Lelj, F. *J. Mol. Struct.: THEOCHEM* **1997**, *389*, 83.
(23) (a) Irigoras, A.; Fowler, J. E.; Ugalde, J. M. *J. Am. Chem. Soc.* **1999**, *121*, 574. (b) Irigoras, A.; Fowler, J. E.; Ugalde, J. M. *J. Am. Chem. Soc.* **1999**, *121*, 8549. (c) Irigoras, A.; Elizalde, O.; Silanes, I.; Fowler, J. E.; Ugalde, J. M. *J. Am. Chem. Soc.* **2000**, *122*, 114.
(24) Klippenstein, S. J.; Yang, C.-N. *Int. J. Mass Spectrom.* **2000**, *201*, 253.
(25) Feller, D.; Glendening, E. D.; de Jong, W. A. *J. Chem. Phys.* **1999**, *110*, 1475.
(26) El-Nahas, A. M. *Chem. Phys. Lett.* **2001**, *345*, 325.
(27) (a) Reinhard, B. M.; Niedner-Schatteburg, G. *J. Phys. Chem. A* **2002**, *106*, 7988. (b) Reinhard, B. M.; Niedner-Schatteburg, G. *Phys. Chem. Chem. Phys.* **2002**, *4*, 1471. (c) Reinhard, B. M.; Niedner-Schatteburg, G. *J. Chem. Phys.* **2003**, *118*, 3571.
(28) Lee, E. C.; Lee, H. M.; Tarakeshwar, P.; Kim, K. S. *J. Chem. Phys.* **2003**, *119*, 7725.
(29) (a) Markham, G. D.; Glusker, J. P.; Bock, C. W. *J. Phys. Chem. B* **2002**, 106, 5118. (b) Bock, C. W.; Markham, G. D.; Katz, A. K.; Glusker, J. P. *Inorg. Chem.* **2003**, *42*, 1538. (c) Trachtman, M.; Markham, G. D.; Glusker, J. P.; George, P.; Bock, C. W. *Inorg. Chem.* **1998**, *37*, 4421.
(30) (a) Shen, M. H.; Farrar, J. M. *J. Chem. Phys.* **1991**, *94*, 3322. (b) Shen, M. H.; Winniczek, J. W.; Farrar, J. M. *J. Phys. Chem.* **1987**, *91*, 6447.
(31) (a) Willey, K. F.; Yeh, C. S.; Robbins, D.; Pilgrim, J. S.; Duncan, M. A. *J. Chem. Phys.* **1992**, *97*, 8886. (b) Scurlock, C. T.; Pullins, S. H.; Reddic, J. E.; Duncan, M. A. *J. Chem. Phys.* **1996**, *104*, 4591. (c) Duncan, M. A. *Annu. Rev. Phys. Chem.* **1997**, *48*, 69.
(32) (a) Sanekata, M.; Misaizu, F.; Fuke, K. *J. Chem. Phys.* **1996**, *104*, 9768. (b) Misaizu, F.; Sanekata, M.; Tsukamoto, K.; Fuke, K.; Iwata, S. *J. Phys. Chem.* **1992**, *96*, 8259. (c) Misaizu, F.; Sanekata, M.; Fuke, K.; Iwata, S. *J. Chem. Phys.* **1994**, *100*, 1161. (d) Sanekata, M.; Misaizu, F.; Fuke, K.; Iwata, S.; Hashimoto, K. *J. Am. Chem. Soc.* **1995**, *117*, 747. (e) Fuke, K.; Hashimoto, K.; Takasu, R. *Adv. Met. Semicond. Clusters* **2001**, *5*, 1.
(33) Lessen, D. E.; Asher, R. L.; Brucat, P. J. *J. Chem. Phys.* **1990**, *93*, 6102.
(34) (a) Faherty, K. P.; Thompson, C. J.; Aquirre, F.; Michne, J.; Metz, R. B. *J. Phys. Chem. A* **2001**, *105*, 10054. (b) Thompson, C. J.; Husband, J.; Aguirre, F.; Metz, R. B. *J. Phys. Chem. A* **2000**, *104*, 8155. (c) Thompson, C. J.; Aguirre, F.; Husband, J.; Metz, R. B. *J. Phys. Chem. A* **2000**, *104*, 9901−9905. (d) Beyer, M. K.; Metz, R. B. *J. Phys. Chem. A* **2003**, *107*, 1760. (e) Metz, R. B. *Int. J. Mass Spectrom.* **2004**, *235*, 131.
(35) Wang, K.; Rodham, D. A.; McKoy, V.; Blake, G. A. *J. Chem. Phys.* **1998**, *108*, 4817.
(36) Agreiter, J. K.; Knight, A. M.; Duncan, M. A. *Chem. Phys. Lett.* **1999**, *313*, 162.
(37) (a) Cabarcos, O. M.; Weinheimer, C. J.; Lisy, J. M. *J. Chem. Phys.* **1999**, *110*, 8429. (b) Cabarcos, O. M.; Weinheimer, C. J.; Lisy, J. M. *J. Chem. Phys.* **1998**, *108*, 5151. (c) Lisy, J. M. *Int. Rev. Phys. Chem.* **1997**, *16*, 267. (d) Weinheimer, C. J.; Lisy, J. M. *J. Chem. Phys.* **1996**, *105*, 2938. (e) Lisy, J. M. In *Cluster Ions*; Ng, C., Baer, T., Powis, I., Eds.; Wiley: Chichester, U.K., 1993; p 217. (f) Vaden, T. D.; Forinash, B.; Lisy, J. M. *J. Chem. Phys.* **2002**, *117*, 4628. (g) Vaden, T. D.; Weinheimer, C. J.; Lisy, J. M. *J. Chem. Phys.* **2004**, *121*, 3102. (k) Patwari, G. N.; Lisy, J. M. *J. Chem. Phys.* **2003**, *118*, 8555.
(38) (a) Walker, N. R.; Walters, R. S.; Pillai, E. D.; Duncan, M. A. *J. Chem. Phys.* **2003**, *119*, 10471. (b) Walters, R. S.; Duncan, M. A. *Aust. J. Chem.* **2004**, *57*, 1145. (c) Walker, N. R.; Walters, R. S.; Tsai, C.-S.; Jordan, K. D.; Duncan, M. A. *J. Phys. Chem. A* **2005**, *109*, 7057.
(39) (a) Inokuchi, Y.; Ohshimo, K.; Misaizu, F.; Nishi, N. *Chem. Phys. Lett.* **2004**, *390*, 140. (b) Inokuchi, Y.; Ohshimo, K.; Misaizu, F.; Nishi, N. *J. Phys. Chem. A* **2004**, *108*, 5034.
(40) (a) Gregoire, G.; Velasquez, J.; Duncan, M. A. *Chem. Phys. Lett.* **2001**, *349*, 451. (b) Gregoire, G.; Duncan, M. A. *J. Chem. Phys.* **2002**, *117*, 2120.
(41) (a) Gregoire, G.; Brinkman, N. R.; Schaefer, H. F.; Duncan, M. A. *J. Phys. Chem. A* **2003**, *107*, 218. (b) Walters, R. S.; Jaeger, T. D.; Brinkman, N. R.; Schaefer, H. F.; Duncan, M. A. *J. Phys. Chem. A* **2003**, *107*, 7396.
(42) (a) Walker, N. R.; Grieves, G. A.; Walters, R. S.; Duncan, M. A. *Chem. Phys. Lett.* **2003**, *380*, 230. (b) Walker, N. R.; Walters, R. S.; Duncan, M. A. *J. Chem. Phys.* **2004**, *120*, 10037. (c) Walker, N. R.; Grieves, G. A.; Walters, R. S.; Duncan, M. A. *J. Chem. Phys.* **2004**, *121*, 10498.
(43) (a) Walters, R. S.; Jaeger, T. D.; Duncan, M. A. *J. Phys. Chem. A* **2002**, *106*, 10482. (b) Walters, R. S.; Schleyer, P. v. R, Corminboeuf, C.; Duncan, M. A. *J. Am. Chem. Soc.* **2005**, *127*, 1100. (c) Pillai, E. D.; Walters, R. S.; Schleyer, P. v. R, Duncan, M. A. To be submitted for publication.
(44) (a) Jaeger, T. D.; Duncan, M. A. *J. Phys. Chem. A* **2004**, *108*, 6605. (b) Jaeger, J. B.; Pillai, E. D.; Jaeger, T. D.; Duncan, M. A. *J. Phys. Chem. A* **2005**, *109*, 2801. (c) Jaeger, T. D.; Duncan, M. A. *J. Phys. Chem. A* **2005**, *109*, 3311.
(45) Pillai, E. D.; Jaeger, T. D.; Duncan, M. A. *J. Phys. Chem. A* **2005**, *109*, 3521.
(46) Duncan, M. A. *Int. Rev. Phys. Chem.* **2003**, *22*, 407.
(47) (a) van Heijnsbergen, D.; von Helden, G.; Meijer, G.; Maitre, P.; Duncan, M. A. *J. Am. Chem. Soc.* **2002**, *124*, 1562. (b) van Heijnsbergen, D.; Jaeger, T. D.; von Helden, G.; Meijer, G.; Duncan, M. A. *Chem. Phys. Lett.* **2002**, *364*, 345. (c) Jaeger, T. D.; van Heijnsbergen, D.; Klippenstein, S.; von Helden, G.; Meijer, G.; Duncan, M. A. *J. Am. Chem. Soc.* **2004**, *126*, 10981.
(48) (a) Oomens, J.; Moore, D. T.; von Helden, G.; Meijer, G.; Dunbar, R. C. *J. Am. Chem. Soc.* **2004**, *126*, 724. (b) Moore, D. T.; Oomens, J.; Eyler, J. R.; Meijer, G.; von Helden, G.; Ridge, D. P. *J. Am. Chem. Soc.* **2004**, *126*, 14726.
(49) (a) Simon, A.; Jones, W.; Ortega, J.-M.; Boissel, P.; Lemaire, J.; Maitre, P. *J. Am. Chem. Soc.* **2004**, *126*, 11666. (b) Le Caer, S.; Heninger, M.; Maitre, P.; Mestdagh, H. *Rapid Commun. Mass Spectrom.* **2003**, *17*, 351. (c) Lemaire, J.; Boissel, P.; Heninger, M.; Mauclaire, G.; Bellec, G.; Mestdagh, H.; Simon, A.; Le Caer, S.; Ortega, J.-M.; Glotin, F.; Maitre, P. *Phys. Rev. Lett.* **2002**, *89*, 273002.
(50) Shimanouchi, T. *Molecular Vibrational Frequencies*, 69th ed.; Chemistry WebBook, NIST Standard Reference Database (http://webbook.nist.gov); NIST: Gaithersburg, MD, 2001.
(51) (a) Pimentel, G. C.; McClellan, A. L. *The Hydrogen Bond*; Freeman: San Francisco, 1960. (b) Pimentel, G. C.; McClellan, A. L. *Annu. Rev. Phys. Chem.* **1971**, *22*, 347.

Lisy and co-workers have investigated the clustering behavior of alkali-metal cation−water complexes and mixed complexes containing water and other solvent molecules using this method.[37] Several other research groups have studied nonmetal anion−water or protonated water complexes using similar methodology.[55−62] In recent experiments by our group and others,[38,39] laser vaporization cluster sources have been incorporated together with IR photodissociation spectroscopy, making it possible to explore small cation−water complexes containing refractory metals. In the present work we present a study of $Ni^+(H_2O)_n$ complexes up to complex sizes of $n = 25$. This is the first study to document the progressive solvation of a transition-metal cation.

Experimental Section

Nickel−water complexes are produced by laser vaporization in a pulsed supersonic expansion and analyzed in a reflectron time-of-flight mass spectrometer. The molecular beam apparatus and the mass spectrometer have been described previously.[38,46] A rotating nickel rod is vaporized by the third harmonic of a Nd:YAG (355 nm) in the source chamber. $Ni^+(H_2O)_n$ clusters are produced by adding a few drops of water to a helium, neon, or argon expansion produced by a pulsed General Valve (1 mm nozzle) at 60 psi backing pressure and 200 μs pulse duration. The ions are skimmed into the mass spectrometer and extracted into the first flight tube of the reflectron using pulsed acceleration voltages. They are then mass-selected by pulsed deflection plates before entering the reflectron where they are excited and photodissociated at the turning point by the infrared output of an optical parametric oscillator (OPO). The characteristics of the OPO have been described previously.[38,40−46] Parent and fragment ions are mass-analyzed in the second flight tube using an electron multiplier tube detector and recorded with a digital oscilloscope (LeCroy LT342). The data are transferred and stored in a PC via an IEEE-488 interface. Infrared resonance-enhanced photodissociation (IR-REPD) spectra are obtained by monitoring the intensity of the fragment ions as a function of the laser wavelength.

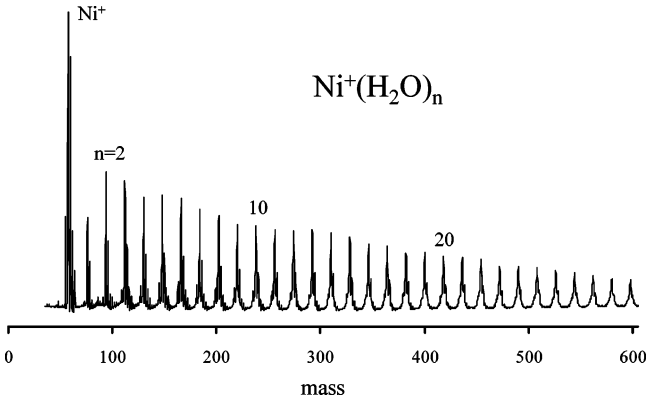

Figure 1. Mass spectrum of $Ni^+(H_2O)_n$ cation clusters produced by laser vaporization.

Density functional theory (DFT) calculations (Gaussian 03W)[63] were carried out at the B3LYP[64] level using the 6-311+G** basis set on the small cation−water complexes $Ni^+(H_2O)_{1-5}$, to elucidate their vibrational band assignments. Vibrational frequencies were scaled by a factor of 0.96, consistent with earlier work on similar systems.[24]

Results and Discussion

Laser vaporization of the nickel sample and coexpansion with water vapor produces a distribution of ion−molecule complexes of the form $Ni^+(H_2O)_n$ extending over the range of about $n = 1-30$, as shown in Figure 1. The multiplet structure on each peak is associated with the naturally occurring isotopes of nickel (58, 60, and 62 amu). This is resolved at low mass, but causes an unresolved width on higher mass peaks. The maximum intensity in this distribution and its extent to higher mass can be adjusted with the partial pressure of water present, by variation of the expansion gas backing pressure or by the impact position and intensity of the vaporization laser on the metal target. The timing of the vaporization laser relative to the beam gas pulse is also an important variable in optimizing this distribution.

To explore the vibrational spectroscopy of these clusters, we size select them one at a time and excite them with the IR OPO to attempt to measure resonance-enhanced photodissociation. When we do this experiment on the small $Ni^+(H_2O)_n$ complexes

(52) Schuster, P., Zundel, G., Sandorfy, C.; Eds. *The Hydrogen Bond: Recent Developments in Theory and Experiments*; North-Holland Publishing Co.: Amsterdam, 1976; Vol. 2.
(53) Jeffrey, G. A. *An Introduction to Hydrogen Bonding*; Oxford University Press: Oxford, U.K., 1997.
(54) Scheiner, S. *Hydrogen Bonding, A Theoretical Perspective*; Oxford University Press: Oxford, U.K., 1997.
(55) (a) Yeh, L. I.; Okumura, M.; Myers, J. D.; Price, J. M.; Lee, Y. T. *J. Chem. Phys.* **1989**, *91*, 7319. (b) Okumura, M.; Yeh, L. I.; Myers, J. D.; Lee, Y. T. *J. Phys. Chem.* **1990**, *94*, 3416. (c) Yeh, L. I.; Lee, Y. T.; Hougen, J. T. *J. Mol. Spectrosc.* **1994**, *164*, 473. (d) Crofteon, M. W.; Price, J. M.; Lee, Y. T. *Springer Ser. Chem. Phys.* **1994**, *56* (Clusters of Atoms and Molecules II), 44. (e) Wu, C. C.; Jiang, J. C.; Boo, D. W.; Lin, S. H.; Lee, Y. T.; Chang, H. C. *J. Chem. Phys.* **2000**, *112*, 176. (f) Jiang, J.-C.; Wang, Y.-S.; Chang, H.-C.; Lin, Sheng H.; Lee, Y. T.; Niedner-Schatteburg, G.; Chang, H.-C. *J. Am. Chem. Soc.* **2000**, *122*, 1398. (g) Chaudhuri, C.; Wang, Y. S.; Jiang, J. C.; Lee, Y. T.; Chang, H. C.; Niedner-Schatteburg, G. *Mol. Phys.* **2001**, *99*, 1161. (h) Lin, C. K.; Wu, C. C.; Wang, Y. S.; Lee, Y. T.; Chang, H. C. *Phys. Chem. Chem. Phys.* **2005**, *7*, 938. (i) Wu, C. C.; Lin, C. K.; Chang, H. C.; Jiang, J. C.; Kuo, J. L.; Klein, M. L. *J. Chem. Phys.* **2005**, *122*, 074315.
(56) (a) Choi, J. H.; Kuwata, K. T.; Haas, B. M.; Cao, Y.; Johnson, M. S.; Okumura, M. *J. Chem. Phys.* **1994**, *100*, 7153. (b) Choi, J. H.; Kuwata, K. T.; Cao, Y. B.; Okumura, M. *J. Phys. Chem. A* **1998**, *102*, 503. (c) Johnson, M. S.; Kuwata, K. T.; Wong, C. K.; Okumura, M. *Chem. Phys. Lett.* **1996**, *260*, 551.
(57) (a) Bailey, C. G.; Kim, J.; Dessent, C. E. H.; Johnson, M. A. *Chem. Phys. Lett.* **1997**, *269*, 122. (b) Ayotte, P.; Weddle, G. H.; Kim, J.; Johnson, M. A. *Chem. Phys.* **1998**, *239*, 485. (c) Ayotte, P.; Weddle, G. H.; Kim, J.; Johnson, M. A. *J. Am. Chem. Soc.* **1998**, *120*, 12361. (d) Ayotte, P.; Bailey, C. G.; Kim, J.; Johnson, M. A. *J. Chem. Phys.* **1998**, *108*, 444. (e) Ayotte, P.; Nielsen, S. B.; Weddle, G. H.; Johnson, M. A.; Xantheas, S. S. *J. Phys. Chem. A* **1999**, *103*, 10665. (f) Price, E. A.; Robertson, W. H.; Diken, E. G.; Weddle, G. H.; Johnson, M. A. *Chem. Phys. Lett.* **2002**, *366*, 412. (g) Corcelli, S. A.; Kelley, J. A.; Tully, J. C.; Johnson, M. A. *J. Phys. Chem. A* **2002**, *106*, 4872. (h) Robertson, W. H.; Johnson, M. A. *Annu. Rev. Phys. Chem.* **2003**, *54*, 173. (i) Robertson, W. H.; Diken, E. G.; Shin, J.-W.; Johnson, M. A. *Science* **2003**, *299*, 1367. (j) Hammer, N. I.; Shin, J.-W.; Headrick, J. M.; Diken, E. G.; Rosciolli, J. R.; Weddle, G. H.; Johnson, M. A. *Science* **2004**, *306*, 675. (k) Price, E. A.; Hammer, N. I.; Johnson, M. A. *J. Phys. Chem. A* **2004**, *108*, 3910. (l) Diken, E. G.; Robertson, W. H.; Johnson, M. A. *J. Phys. Chem. A* **2004**, *108*, 64. (m) Headrick, J. M.; Bopp, J. C.; Johnson, M. A. *J. Chem. Phys.* **2004**, *121*, 11523.
(58) (a) Sawamura, T.; Fujii, A.; Sato, S.; Ebata, T.; Mikami, N. *J. Phys. Chem.* **1996**, *100*, 8131. (b) Ebata, T.; Fujii, A.; Mikami, N. *Int. Rev. Phys. Chem.* **1998**, *17*, 331. (c) Miyazaki, M.; Fujii, A.; Ebata, T.; Mikami, N. *Science* **2004**, *304*, 1134. (d) Miyazaki, M.; Fujii, A.; Ebata, T.; Mikami, N. *J. Phys. Chem. A* **2004**, *108*, 10656. (e) Miyazaki, M.; Fujii, A.; Ebata, T.; Mikami, N. *Phys. Chem. Chem. Phys.* **2003**, *5*, 1137. (f) Miyazaki, M.; Fujii, A.; Ebata, T.; Mikami, N. *Science* **2004**, *304*, 1134.
(59) (a) Bieske, E. J.; Dopfer, O. *Chem. Rev.* **2000**, *100*, 3963. (b) Dopfer, O.; Roth, D.; Maier, J. P. *J. Phys. Chem. A* **2000**, *104*, 11702. (b) Dopfer, O.; Roth, D.; Maier, J. P. *J. Chem. Phys.* **2001**, *114*, 7081.
(60) (a) Lehr, L.; Zanni, M. T.; Frischkorn, C.; Weinkauf, R.; Neumark, D. M. *Science* **1999**, *284*, 635. (b) Asmis, K. R.; Pivonka, N. L.; Santambrogio, G.; Bruemmer, M.; Kaposta, C.; Neumark, D. M.; Woeste, L. *Science* **2003**, *299*, 1375.
(61) (a) Shin, J.-W.; Hammer, N. I.; Diken, E. G.; Johnson, M. A.; Walters, R. S.; Jaeger, T. D.; Duncan, M. A.; Christie, R. A.; Jordan, K. D. *Science* **2004**, *304*, 1137. (b) Headrick, J.; Diken, E. G.; Walters, R. S.; Hammer, N. I.; Christie, R. A.; Cui, J.; Myshakin, E. M.; Duncan, M. A.; Johnson, M. A.; Jordan, K. D. *Science* **2005**, *308*, 1765.
(62) Fridgen, T. D.; McMahon, T. B.; MacAleese, L.; Lemaire, J.; Maitre, P. *J. Phys. Chem. A* **2004**, *108*, 9008.
(63) Frisch, M. J.; et al. *Gaussian 03*, rev. B.02; Gaussian, Inc.: Pittsburgh, PA.
(64) (a) Becke, A. D. *J. Chem. Phys.* **1993**, *98*, 5648. (b) Lee, C.; Yang, W.; Parr, R. G. *Phys. Rev. B* **1988**, *37*, 785.

Table 1. Dissociation Energies of $Ni^+(H_2O)_n$ Ions (kcal/mol)

	experimental	theoretical
$Ni^+(H_2O)$	39.7,[a] 36.5,[b] 43.9[c]	41.9,[d] 45.0[e]
$Ni^+(H_2O)_2$	38.0,[b] 40.6,[a] 40.2[c]	
$Ni^+(H_2O)_3$	16.2[c]	
$Ni^+(H_2O)_4$	12.3[c]	

[a] Reference 8. [b] Reference 9. [c] Reference 10. [d] Reference 20. [e] Reference 24.

($n = 1-2$), we can detect no measurable photodissociation signal in the vicinity of the O−H stretches of water. This is not surprising, because photodissociation requires that the IR excitation provide enough energy to break a bond in the cluster. The weakest bond in cation−water complexes is expected to be that between the metal ion and the water molecules. The dissociation energies of $Ni^+(H_2O)_{1-4}$ ions have been measured previously via collision-induced dissociation experiments,[8−10] and the binding energies in these ions have also been computed.[20,23,24] These values are reported in Table 1. As shown, the binding energy of the last water molecule in each of these complexes exceeds 12 kcal/mol (about 4000 cm^{-1}), and therefore, it is understandable that our IR excitation near 3600−3700 cm^{-1} is not energetic enough to break such a bond to eliminate water from these clusters. As in many ion−molecule complexes, the average binding energies for water molecules beyond the first in this system decrease with cluster size. The binding energies of the $n = 1$ and 2 complexes are quite similar, and there is a sharp decrease noticeable on going from the $n = 2$ to $n = 3$ complex. The $n = 3$ and 4 complex binding energies are close to the IR photon energy in the O−H stretching region, but still slightly greater.

To obtain a spectrum for the $n = 1$ complex, we employ the method of "rare gas tagging".[38−46,57−59] This general method was first known as "spectator" atom or molecule attachment, as described by Lee and co-workers.[55] It is now a common method of measurement for photodissociation spectroscopy of ion−molecule complexes. To do this, we produce mixed complexes of the form $Ni^+(H_2O)(Ar)_m$ by making the ions in an expansion of argon. The binding energy of argon to many ion−molecule complexes is low enough so that photoexcitation in the IR can lead to argon elimination. If the argon is relatively weakly bound and attached at a binding site remote from the chromophore of interest, then this tagging method can provide an IR photodissociation spectrum whose resonances lie very close (5−10 cm^{-1}) to those of the parent ion of interest. The binding energy of argon to the nickel cation in the Ni^+Ar diatomic molecule is 4572 ± 5 cm^{-1}.[65c] Consistent with a similar high binding energy for the argon in the mixed complex, we find that we also cannot dissociate $Ni^+(H_2O)Ar$ in the O−H stretch region. However, we are able to produce the complex $Ni^+(H_2O)Ar_2$, and this ion does dissociate by losing argon. Apparently, the binding energy of the second argon is lower than the IR excitation energy, because the dissociation is efficient. Unfortunately, we cannot produce the $Ni^+(H_2O)_2Ar$ complexes or larger complexes tagged with argon having enough intensity to study. The tagging experiment is therefore only useful to examine the spectrum of the monohydrated complex.

(65) (a) Lessen, D. E.; Brucat, P. J. *Chem. Phys. Lett.* **1988**, *152*, 473. (b) Lessen, D. E.; Asher, R. L.; Brucat, P. J. *Adv. Met. Semicond. Clusters* **1993**, *1*, 267. (c) Asher, R. L.; Bellert, D.; Buthelezi, T.; Brucat, P. J. *Chem. Phys. Lett.* **1994**, *228*, 599.

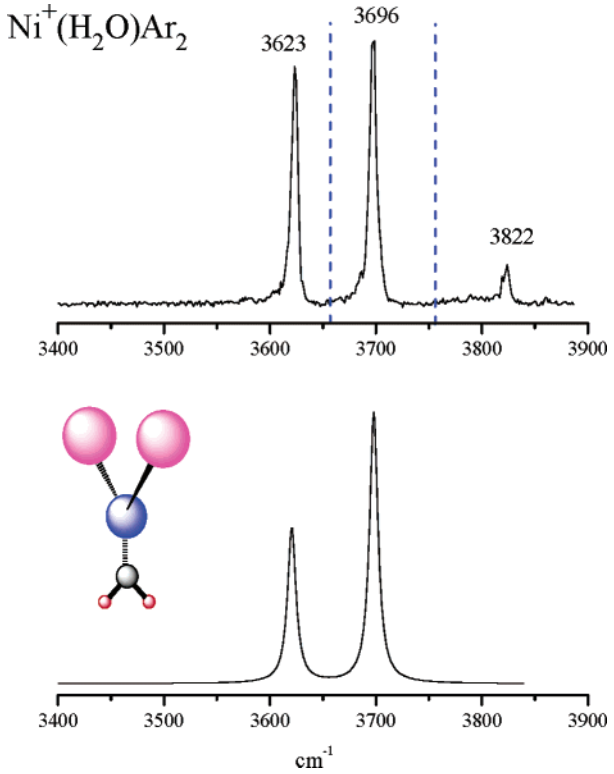

Figure 2. Infrared photodissociation spectrum of $Ni^+(H_2O)Ar_2$ measured in the loss of argon channel. The lower trace is the spectrum predicted with B3LYP/6-311+G**.

The spectrum that we measure for $Ni^+(H_2O)Ar_2$ in the loss of argon channel is shown in Figure 2. There are two strong resonances measured at 3623 and 3696 cm^{-1}, and there is a much weaker band at 3822 cm^{-1}. Spectra similar to this one have been reported recently by our group for the corresponding $V^+(H_2O)$ and $Fe^+(H_2O)$ species.[38a,b] Both our group[38c] and that of Nishi and co-workers[39] have studied $Mg^+(H_2O)$, where a similar spectrum is also observed. The IR-active fundamentals expected in this wavelength region are those corresponding to the symmetric and asymmetric stretching modes of the free water molecule. These frequencies (3657 and 3756 cm^{-1}) are shown with the blue dashed lines in the figure. As indicated, the two most intense bands in the present spectrum appear at frequencies just lower than those of the free water vibrations. We therefore assign the 3623 cm^{-1} band as the symmetric stretch and the 3696 cm^{-1} band as the asymmetric stretch. The red shifts are then 34 and 60 cm^{-1}, respectively, for these transitions relative to those in the free water molecule. The weaker band at 3822 cm^{-1} is also seen frequently in the spectra of other water-containing clusters, and it is generally assigned to be a combination band between one of the O−H stretch vibrations and an intermolecular stretch or bend. For example, this band lies 199 cm^{-1} above the symmetric stretch band, and an in-plane bend is predicted at 189 cm^{-1}.

To make a more quantitative investigation of this spectrum, we have performed DFT calculations on the $Ni^+(H_2O)$ complex with zero, one, and two argons attached, and these data are presented in Table 2. The $Ni^+(H_2O)$ complex is bound in a C_{2v} configuration consistent with a significant charge-dipole component in its bonding, as expected. The first argon atom is added opposite the water on the C_2 axis, preserving the C_{2v} symmetry. When two argons are present, they bind opposite each other

Table 2. Structural Data and Vibrational Frequencies Calculated for the Various $Ni^+(H_2O)_n$ Complexes at the B3LYP/6-311+G** Level[a]

complex	structure	energies (kcal/mol), BE[b] (D_e)[c]	selected frequencies (cm^{-1}) (IR intensities, km/mol)	M^+–O (Å)	M^+–Ar (Å)
$Ni^+(H_2O)$	$^2B_2$ (C_{2v})	39.0 (39.0)	1585 (87), 3620 (148), 3695 (267)	2.002	
$Ni^+(H_2O)Ar$	$^2B_2$ (C_{2v})	52.1 (43.0) (13.0)	1596 (84), 3628 (156), 3704 (255)	1.948	2.333
$Ni^+(H_2O)Ar_2$	$^2B_2$ (C_{2v})	57.5 (38.3) (5.4)	1587 (90), 3621 (137), 3698 (237)	1.966	2.477
$Ni^+(H_2O)_2$	^2B (C_2)	86.3 (47.3)	1586 (19), 1586 (177), 3622 (280), 3625 (0.5), 3699 (33), 3700 (466)	1.913	
$Ni^+(H_2O)_3$	$^2A_1$ (C_{2v})	108.3 (22)	1581 (125), 1582 (150), 1583 (6), 3641 (155), 3642 (42), 3651 (60), 3722 (0), 3723 (390), 3738 (166)	2.003, 2.003, 2.047	
$Ni^+(H_2O)_4$	^2B (C_2)	125.0 (16.7)	1569 (154), 1574 (28), 1574 (40), 1578 (146), 3638 (28), 3640 (85), 3644 (79), 3645 (20), 3724 (8), 3725 (286), 3734 (105), 3734 (190)	2.079, 2.079, 2.106, 2.106	
$[Ni^+(H_2O)_3](H_2O)$	$^2A'$ (C_s)	123.0 (14.7)	1569 (114), 1577 (94), 1580 (85), 1608 (32), 3292 (1201), 3642 (104), 3645 (55), 3656 (39), 3719 (117), 3724 (148), 3728 (211), 3746 (138)	2.031, 1.996, 2.007, 4.245	
$[Ni^+(H_2O)_4](H_2O)$	^2A (C_1)	141.0 (16.1)	1568 (121), 1571 (92), 1573 (114), 1579 (26), 1608 (57), 3485 (110), 3516 (736), 3633 (30), 3638 (45), 3643 (49), 3699 (141), 3708 (131), 3715 (142), 3725 (154), 3734 (137)	2.124, 2.074, 2.075, 2.096, 3.848	
$[Ni^+(H_2O)_3](H_2O)_2$	^2A (C_1)	138.0 (14.8)	1567 (124), 1573 (84), 1575 (79), 1601 (62), 1604 (28), 3258 (1391), 3335 (921), 3647 (64), 3655 (38), 3661 (40), 3709 (121), 3721 (114), 3731 (169), 3746 (133), 3752 (137)	2.001, 2.027, 1.986, 4.267, 4.149	
$Ni^+(H_2O)_3](H_2O)_2$	$^2A_1$ (C_{2v})	135.1 (12.1)	1566 (143), 1572 (18), 1573 (200), 1575 (1), 1620 (7), 3395 (636), 3442 (1198), 3647 (126), 3648 (0), 3656 (15), 3657 (45), 3732 (0), 3732 (322), 3746 (0), 3747 (253)	2.016, 2.016, 1.993, 4.189, 4.189	

[a] A full description of our DFT calculations, including a complete list of all the vibrational frequencies, is given in the Supporting Information for this paper. Vibrations are scaled by 0.96.[24] [b] Total binding energy for all ligands in the cluster relative to separated M^+ and $n(H_2O) + m$Ar. [c] Dissociation energy for elimination of the "last" ligand. In the case of argon-tagged species, the first number in parentheses is the energy for the last water and the second is that for the argon.

and off the C_2 axis, with each out of the plane formed by the cation + water, but again preserving the overall C_{2v} symmetry. These calculations find symmetric and asymmetric stretches for the $Ni^+(H_2O)$ ground-state $^2B_2$ complex (scaled by 0.96) of 3620 and 3695 cm^{-1}, while those for the complex tagged with one and two argons are 3628/3704 and 3621/3698 cm^{-1}, respectively. The argon atoms reduce the red shift of the O−H stretches compared to the values for the isolated $Ni^+(H_2O)$ complex. This indicates that the argon atoms act essentially as ligands, partially diluting the red shift expected for the isolated $Ni^+(H_2O)$ complex. Figure 2 shows the spectrum calculated for the $Ni^+(H_2O)Ar_2$ complex compared to the experimental one. The agreement between the band positions predicted by theory and those measured by the experiment is excellent when the argon atoms are included. Although the band positions match well, the relative intensities are somewhat different between the predicted *absorption* spectrum and the measured *photodissociation* spectrum. This difference could arise from different dissociation yields for the two vibrational modes or simply because the measured spectrum is partially saturated, which would enhance the intensity of the weaker band. It is not possible to explain line intensities completely, and therefore, we focus primarily on band positions in the subsequent discussion.

Red-shifted O−H stretching modes have now been seen in the spectra of all the $M^+(H_2O)$ complexes that have been studied.[37−39] We have explained this shift previously in terms of an inductive effect in which the metal cation binds in a C_{2v} configuration with water, attached in the region of the lone pair electrons, and polarizes these electrons. The lone pair electrons have partial bonding character, and as this electron density is shifted away from the water, its bonding is disrupted. Weaker bonding on the water subsystem leads to lower frequency vibrations, explaining the observed red shifts. Also consistent with this reasoning, the OH stretches in the H_2O^+ ion are 3213 and 3259 cm^{-1}, and these are >400 cm^{-1} red-shifted compared to those of neutral water.[50] Although the details of the orbitals are different, the red-shifting of vibrations here is similar to that found for the carbonyl stretch in $M(CO)_n$ complexes, which comes from the familiar effects of σ-donation and π-back-bonding.[66,67] We have recently seen a similar red shift for the C−H stretches in $M^+(C_2H_2)_n$ complexes[43] and for the N−N stretch in $M^+(N_2)_n$ complexes.[45]

As noted above, we are not able to produce enough argon-tagged $Ni^+(H_2O)_2$ or larger complexes for study. However, we have calculated the structure for the $n = 2$ complex, and we find that the two water molecules bind opposite each other in an overall C_2 configuration, very close to the planar D_{2h} structure. As shown in Table 2, these O−H stretches for $Ni^+(H_2O)_2$ are predicted to be red-shifted a little less than those for $Ni^+(H_2O)$.

We find that photodissociation becomes possible for the $n = 3$ and larger complexes without the need for tagging. This is initially a surprise, because the binding energies in the $n = 3$ and 4 complexes are still slightly higher than the energies of vibrations in the O−H stretching region. However, the energetics are close, and it is reasonable that some fraction of the clusters produced have internal energy that is not completely quenched in the supersonic expansion. If the $n = 3$ and 4 complexes contain a few hundred inverse centimeters of internal energy prior to excitation with the infrared laser, it is possible that dissociation can occur. Likewise, it is conceivable that there is

(66) Frenking, G.; Froelich, N. *Chem. Rev.* **2000**, *100*, 717.
(67) Zhou, M.; Andrews, L.; Bauschlicher, C. W., Jr. *Chem. Rev.* **2001**, *101*, 1931.

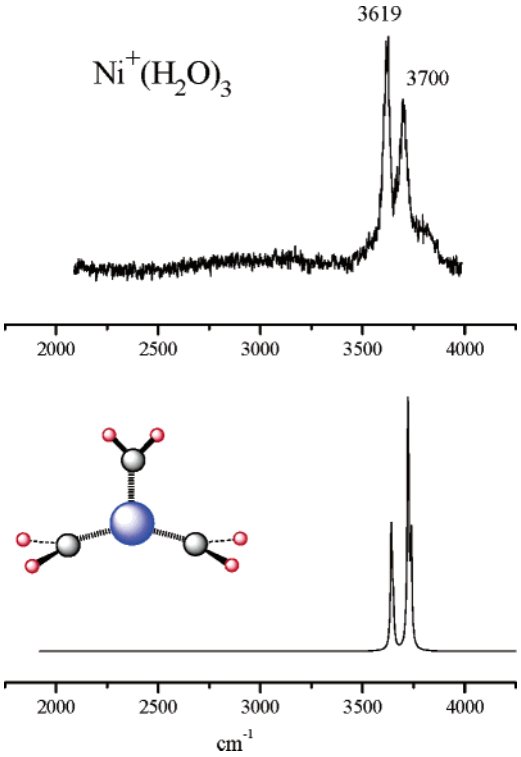

Figure 3. Infrared photodissociation spectrum of $Ni^+(H_2O)_3$ measured in the loss of water channel (top) compared to the spectrum predicted by theory (bottom).

a small amount of two-photon absorption that allows these complexes to be studied. In any event, we can measure spectra for the $n = 3$ and larger complexes all the way up to $n = 25$. All these spectra are recorded in the mass channel corresponding to the loss of one water molecule from the selected parent ion.

Figure 3 shows the spectrum for the $Ni^+(H_2O)_3$ complex, which is the smallest one that we can measure without argon tagging. As shown, there are again resonances in the O−H stretch region near the frequencies of the free water molecule. Two broad bands are observed at 3619 and 3700 cm^{-1}, which are red-shifted 38 and 56 cm^{-1} from the free water vibrations. The width of these features presumably occurs because clusters with elevated internal energy are detected preferentially in this experiment, and those species would have thermal (rotational or sequence band structure) width on their bands. A broad shoulder on the high-frequency side of the spectrum may come from an unresolved combination band like that seen at 3822 cm^{-1} for the $n = 1$ species. If we allow for some uncertainty in band positions due to the width of these features, then the red shifts for the $n = 3$ complex are essentially the same as those of the $Ni^+(H_2O)Ar_2$ complex. Even though the argon binding is weaker, both complexes have three ligands to distribute the binding interactions, and it is perhaps understandable that the red shifts are not so different. There is no signal in the lower frequency region (3200−3500 cm^{-1}) where resonances from hydrogen-bonded water molecules might be found. We therefore conclude that all three water molecules in these complexes are coordinated directly to the metal ion, with all O−H groups pointing away from the metal so that they vibrate freely.

We have also calculated the structure and spectrum for the $n = 3$ complex, and these results are presented in Table 2 and Figure 3. We find only one stable isomer for the structure of this complex. Consistent with our interpretation of the spectral shifts, all three water molecules are attached directly to the metal cation. Two waters have their hydrogens opposite each other and out of the O−Ni^+−O plane, while the third water has its hydrogens in this plane, yielding an overall C_{2v} configuration. Red-shifted O−H vibrations, consistent with the experimental observations, are again predicted. The calculated spectrum is also shown in Figure 3, and its band positions agree nicely with the experiment.

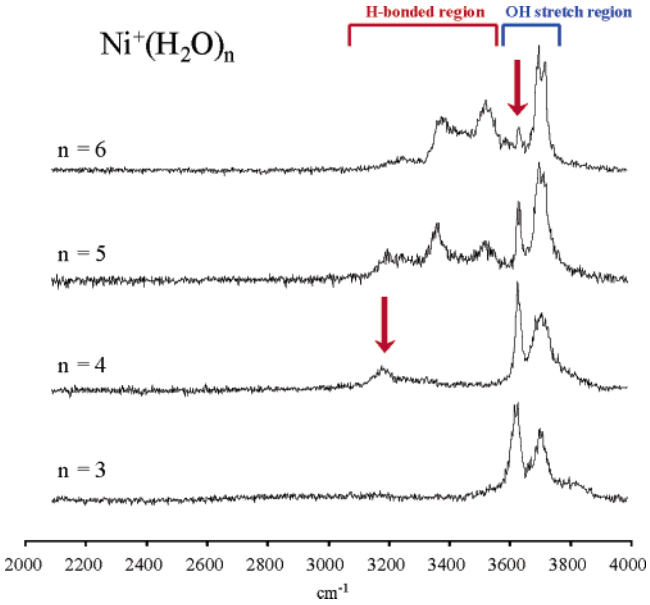

Figure 4. IR photodissociation spectra of the $Ni^+(H_2O)_n$ complexes for $n = 3-6$.

Figure 4 shows a comparison of the spectrum measured for the $Ni^+(H_2O)_3$ complex to those of the next larger $n = 4$, 5, and 6 species. Vibrational band positions for these and the other clusters studied here are presented in Table 3. Resonances are detected for all of these species in the region of the O−H stretching vibrations (3600−3800 cm^{-1}) like those seen for the $n = 1$ and $n = 3$ species. The spectra for the larger clusters here are broad and are more like the $n = 3$ spectrum than they are like the argon-tagged $n = 1$ spectrum. The $n = 3$ and 4 spectra have similar peak widths, positions, and relative intensities for the two bands, with the symmetric stretch band appearing slightly more narrow and a little more intense than that for the asymmetric stretch. The bands at 3619 and 3700 cm^{-1} for the $n = 3$ complex have shifted only slightly to appear at 3626 and 3702 cm^{-1} for the $n = 4$ complex. The $n = 5$ and 6 spectra in this region begin to change in their relative intensity ratios, with the lower frequency band decreasing in intensity relative to the higher frequency one. At $n = 6$, the lower frequency band (marked with an arrow) has dropped to a barely detectable level, while the higher frequency band has grown narrower and has split into a closely spaced doublet. While these changes evolve in the O−H stretching region, new structure also emerges in the hydrogen-bonding region (3200−3500 cm^{-1}). The first sign of any resonances here comes for the $n = 4$ complex, which has a single band near 3180 cm^{-1}. The $n = 5$ spectrum has three bands in this region (3195, 3357, and 3520 cm^{-1}). The $n = 6$ spectrum has bands at 3380 and 3520 cm^{-1} that line up close to the two higher frequency bands seen

Table 3. Band Positions of the Infrared Resonances Measured for $Ni^+(H_2O)_n$ Complexes[a]

$Ni^+(H_2O)Ar_2$	3623, 3696, 3822
$Ni^+(H_2O)_3$	3619, 3700
$Ni^+(H_2O)_4$	3180, 3626, 3702
$Ni^+(H_2O)_5$	3195, 3357, 3520, 3630, 3705
$Ni^+(H_2O)_6$	3380, 3520, 3634, 3694, 3716
$Ni^+(H_2O)_7$	3391, 3526, 3615, 3692, 3721
$Ni^+(H_2O)_8$	3402, 3620, 3694, 3722
$Ni^+(H_2O)_9$	3420, 3520, 3620, 3696, 3722
$Ni^+(H_2O)_{10}$	3520, 3692, 3719
$Ni^+(H_2O)_{11}$	3500, 3698, 3720
$Ni^+(H_2O)_{12}$	3500, 3695, 3719
$Ni^+(H_2O)_{13}$	3350, 3500, 3700, 3720
$Ni^+(H_2O)_{14}$	3350, 3510, 3701, 3717
$Ni^+(H_2O)_{15}$	3200, 3360, 3516, 3698, 3718
$Ni^+(H_2O)_{16}$	3514, 3701, 3717
$Ni^+(H_2O)_{17}$	3510, 3701, 3719
$Ni^+(H_2O)_{18}$	3510, 3700, 3720
$Ni^+(H_2O)_{19}$	3510, 3700, 3720
$Ni^+(H_2O)_{20}$	3513, 3700, 3720
$Ni^+(H_2O)_{21}$	3515, 3700, 3720
$Ni^+(H_2O)_{22}$	3515, 3700, 3720
$Ni^+(H_2O)_{23}$	3509, 3698, 3720
$Ni^+(H_2O)_{24}$	3500, 3700, 3720
$Ni^+(H_2O)_{25}$	3500, 3699, 3717
$Ni^+(H_2O)_{26}$	3500, 3698, 3718
$Ni^+(H_2O)_{28}$	−,[b] 3698, 3718
$Ni^+(H_2O)_{30}$	−,[b] 3698, 3719

[a] All units are in cm^{-1}. [b] No measurements were taken in the hydrogen bonding region for these complexes.

for $n = 5$, while the lower frequency band seen for $n = 4$ (3185 cm^{-1}) and 5 (3195 cm^{-1}) has dropped almost out of sight by $n = 6$.

The growth of these clusters clearly has a strong influence on the infrared resonances, and these resonances can be used to understand the cluster growth. The first issue in the small clusters is the identification of the number of molecules in the first coordination sphere. Our previous work with $Ni^+(CO_2)_n$ and $Ni^+(C_2H_2)_n$ complexes[42,43] found clear evidence in the fragmentation patterns and the appearance of new IR bands for a coordination number of four ligands around the singly charged nickel cation under similar gas-phase conditions. A coordination number of four is also not unusual for Ni(I) in conventional inorganic chemistry.[68] However, in the present system, the evidence for coordination is not so clear. These clusters dissociate by the loss of one or two water molecules at all cluster sizes. There is no evidence for a termination point in the fragmentation pattern at a specific cluster size like we saw in the CO_2 and acetylene cluster systems with Ni^+. This is most likely because the bonding energies in these water clusters are still significant in the second and outer layers (1−3 hydrogen bonds at about 5 kcal/mol each; 5 kcal/mol = 1750 cm^{-1}), while the van der Waals bonding in the outer layers of $Ni^+(CO_2)_n$ and $Ni^+(C_2H_2)_n$ clusters was much weaker, allowing multiple ligands to be eliminated from each IR photon absorbed. The first evidence for second-sphere water comes from the appearance of the broad, red-shifted vibrational band in the spectrum of the $n = 4$ cluster at 3180 cm^{-1} (see the red arrow in Figure 4). As noted before, hydrogen bonding causes such red shifts in the O−H stretching vibrations, and the occurrence of a band in this frequency region is good evidence that there is hydrogen bonding in at least some of the clusters at this size, requiring at least one molecule of water that is not attached to metal and is instead in the second sphere.

(68) Cotton, F. A.; Wilkinson, G. W. *Advanced Inorganic Chemistry*; Wiley: New York, 1988.

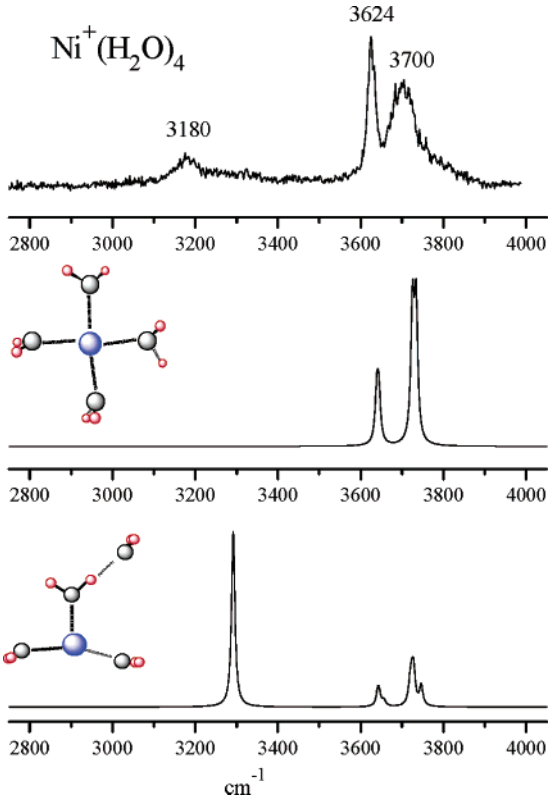

Figure 5. Schematic representations of the different possible configurations for an $n = 4$ complex and the spectra resulting from these compared to the experimental spectrum.

We have calculated the structures and spectra for the $n = 4$ cluster with four ligands coordinated directly to the metal, and the stable configuration has a structure that is nearly square planar with respect to the O atoms. The spectrum for this four-coordinate species is shown in Figure 5, where it is compared to an expanded view of the measured spectrum. As shown, the free OH region matches the experiment, but there is of course no resonance in the hydrogen-bonding region for this species. There are several possible hydrogen-bonding configurations for an $n = 4$ cluster with one external water (i.e., a so-called "3 + 1" species). We can imagine three structures with the external water molecule bridging across two of the inner water molecules, in a "double-donor" (DD) hydrogen-bonding configuration, a "double-acceptor" (AA) configuration, or a "single-donor/single-acceptor" (AD) configuration. However, we have investigated these with theory, and find that none of these bridging structures produce stable minima. Instead, we find that a structure with the one external molecule in a dangling single-acceptor hydrogen-bonding configuration is the only stable configuration for this species. Figure 5 also shows the comparison of the spectrum calculated for this 3 + 1 species to the experimental measurement. Such a structure yields a single kind of hydrogen bond, with a resonance predicted at 3292 cm^{-1}. This is only slightly higher than the measured band at 3180 cm^{-1}. We can therefore conclude that the spectrum for the $n = 4$ complex provides good evidence for the presence of a 3 + 1 structure in this single-acceptor configuration.

It is important to note that the $n = 4$ spectrum does not require *all* of the complexes this size to have such a 3 + 1 configuration.

Isomers in cluster growth have been seen for all the metal−water species studied previously, and the coexistence of isomers is also likely here. Because the previous work in our laboratory found a strong propensity for Ni^+ to have a coordination number of four, it is expected that at least some of the $n = 4$ species have all the water molecules attached directly to the metal. However, as shown in Table 2, the 3 + 1 and the four-coordinate isomers for $Ni^+(H_2O)_4$ are calculated to have virtually the same overall binding energies. The resonances for both species would overlap in the O−H stretching region. The hydrogen-bonding resonance at 3292 cm^{-1} is calculated to have higher IR intensity than bands in the free OH region. Likewise, the spectrum of the 3 + 1 species may appear more intense in these photodissociation spectra because such isomers have a more weakly bound external molecule and are easier to photodissociate. The spectrum is therefore completely consistent with the presence of both the 3 + 1 and four-coordinate isomers for the $n = 4$ complex. However, the hydrogen-bonding band indicates that at least some of the clusters this size have at least one molecule in the second sphere, and we presume that these are the 3 + 1 species found by theory. $n = 4$ is the smallest cluster that provides any evidence for water in the second sphere.

Theory suggests that the three-coordinate and four-coordinate species are comparable energetically, and the spectra are consistent with the presence of both of these in this experiment for the clustering of water around Ni^+. This behavior is quite different from the clustering of CO_2 or acetylene around Ni^+, which we have studied previously.[42,43] In those experiments, there was a sharp preference for a coordination of four, and there was no evidence at all for a coordination of three. These trends are understandable on the basis of the ligand sizes and the ligand−ligand binding energies that contribute to the overall stability of these clusters. Ligands such as CO_2 and acetylene are more compact and therefore fit spatially around a cation more easily than water. Additionally, when there is an external ligand bound to inner-sphere ones, its contribution to the overall stability of the cluster depends on the ligand−ligand binding energy. If we use the molecular dimer binding energies to estimate this, the values for CO_2 (∼500 cm^{-1})[69] and acetylene (∼400 cm^{-1})[70,71] are much lower than that for water (∼1800 cm^{-1}).[51−54] A second-sphere water molecule is then much more strongly bound than a second-sphere CO_2 or acetylene, and it is understandable that structures with external water could be energetically more favored at smaller cluster sizes. Iwata has found evidence for low cation coordination numbers in previous calculations on $M^+(H_2O)_n$ for magnesium and aluminum,[21] and Nishi and co-workers have recently found spectroscopic evidence for this in these systems.[39]

The $n = 5$ spectrum has a much more complex pattern than that seen for the $n = 4$ species. The free OH bands occur at roughly 3630 and 3705 cm^{-1}, and there are three noticeable bumps in the hydrogen-bonding region at approximately 3195, 3357, and 3520 cm^{-1}. As before, resonances in this region indicate the presence of second-sphere water. The additional

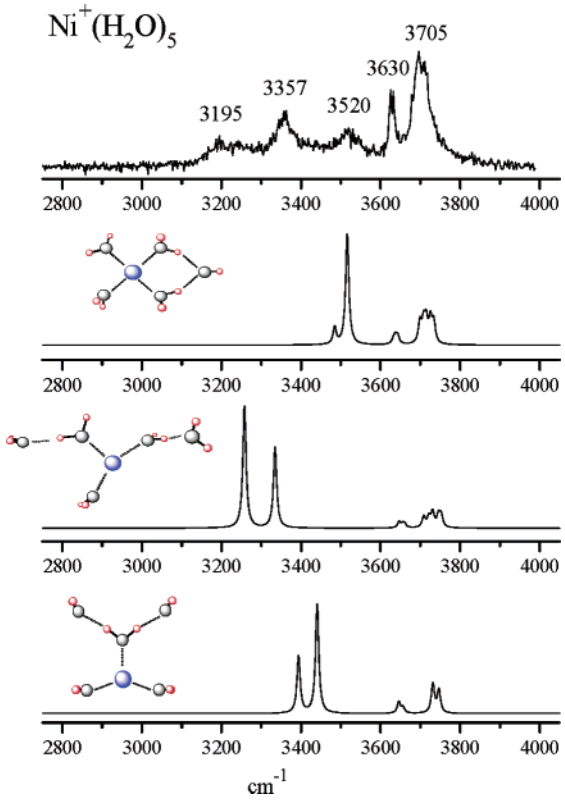

Figure 6. Experimental spectrum for the $n = 5$ cluster compared to those calculated for different isomeric structures. The structures predicted are shown as insets.

structure in this lower frequency region suggests the presence of more than one hydrogen-bonding configuration. If we recall that the 3 + 1 and four-coordinate isomers for the $Ni^+(H_2O)_4$ complex have virtually the same calculated energy, it is then reasonable to consider both 3 + 2 and 4 + 1 isomeric structures for the $Ni^+(H_2O)_5$ complex. We have investigated these with theory, as presented in Table 2 and Figure 6. As indicated, we have found stable structures for a 4 + 1 complex with the external molecule in an "AA" configuration, bridging two inner-sphere molecules, and for two different 3 + 2 structures. One of these 3 + 2 structures (C_1 symmetry) has the two external water molecules accepting a hydrogen bond from two separate inner-sphere molecules, while the other (C_{2v} symmetry) has both external molecules in an accepting configuration from the same inner-sphere molecule. The energy ordering of these is (lowest → highest) 4 + 1, 3 + 2 (C_1), and 3 + 2 (C_{2v}). The hydrogen-bonding resonance predicted for the 4 + 1 species lies at 3516 cm^{-1}, in good agreement with the measured band at 3520 cm^{-1}. The 3 + 2 (C_1) species has two predicted resonances at 3258 and 3335 cm^{-1}, in reasonable agreement with bands measured at 3195 and 3357 cm^{-1}. However, the bands predicted for the 3 + 1 (C_{2v}) species at 3395 and 3442 cm^{-1} are not close to any of the bands measured. Although the resonances are broad and there is considerable uncertainty about this, it is clear that no single one of the low-lying isomers can explain all the measured bands. It seems likely that both the 4 + 1 and 3 + 2 (C_1) isomers are present, and we cannot rule out some contribution from other species such as the 3 + 2 (C_{2v}) isomer. Thus, multiple isomers are necessary to explain the $n = 5$ spectrum, and we can anticipate that the same will be true for all the larger clusters.

(69) Bukowski, R.; Sadlez, J.; Jeziorski, B.; Jankowski, P.; Szalewicz, K.; Kucharski, S. A.; Williams, H. L.; Rice, B. M. *J. Chem. Phys.* **1999**, *110*, 3785.
(70) Alberts, I. L.; Rowlands, T. W.; Handy, N. C. *J. Chem. Phys.* **1988**, *88*, 3811.
(71) (a) Fischer, G.; Miller, R. E.; Vohralik, P. F.; Watts, R. O. *J. Chem. Phys.* **1985**, *83*, 1471. (b) Miller, R. E.; Vohralik, P. F.; Watts, R. O. *J. Chem. Phys.* **1984**, *80*, 5453.

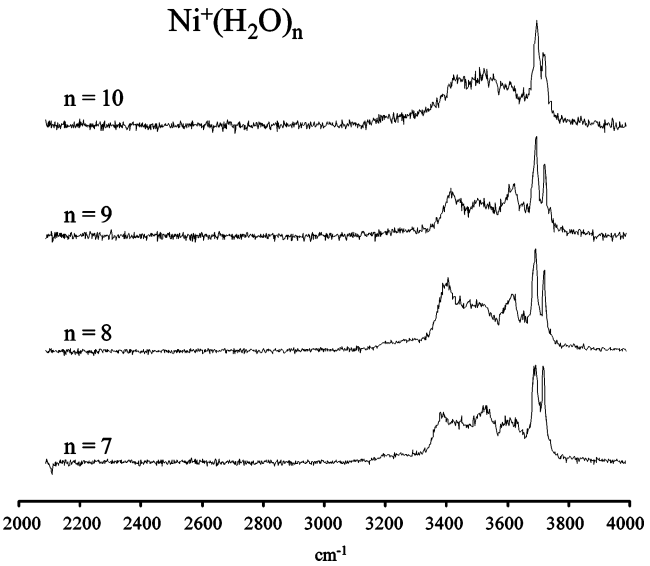

Figure 7. IR photodissociation spectra of the $Ni^+(H_2O)_n$ complexes for $n = 7-10$.

It is interesting to note that the $4 + 1$ structure has the highest hydrogen-bonding OH stretching frequency, and this corresponds to a hydrogen bond with higher connectivity than in the other structures. Two water molecules each provide a donor OH to a single water molecule in a double-acceptor configuration, making a ring structure. The (C_{2v}) $3 + 2$ structure has a single water donating to two acceptors, and it has predicted resonances that are also close to the ones for the $4 + 1$ structure. This is in contrast to the (C_1) $3 + 2$ structure, which has a more open structure with separated hydrogen bonds and lower hydrogen-bonding frequencies. This suggests that hydrogen bonds in more highly connected structures will occur in general at higher frequencies than those in structures with dangling water molecules. Chang and co-workers found a similar trend in their study of protonated water clusters.[55e−i]

Both Figures 5 and 6 show that there is multiplet structure predicted in the region of the free OH stretches (both symmetric and asymmetric). This occurs for structures that have different water molecules that are coordinated directly to the metal versus those in the second coordination layer. Because the binding sites for these molecules are different, it is understandable that inductive effects could lead to their having slightly different OH stretching frequencies. We describe below how a similar effect leads to a well-defined doublet for the asymmetric stretch in larger clusters that have only outer-sphere binding.

Figures 4 and 7 show the continuing evolution of the spectra as the cluster size increases beyond $n = 5$ up to $n = 10$. The positions of bands in these and all the other spectra are given in Table 3. In all of these spectra, there are still resonant features in the region of the free OH and hydrogen-bonded stretches, but the relative intensities and the profiles of the spectra in these regions vary gradually with cluster size. In the free OH region, the small clusters have a sharper, more intense band near 3600 cm^{-1} associated with the symmetric stretch, while the 3700 cm^{-1} band associated with the asymmetric stretch is broader and less intense. In the $n = 4-6$ range, this intensity pattern changes, as the 3600 cm^{-1} feature drops abruptly in intensity, becoming barely noticeable at $n = 6$. The 3700 cm^{-1} band grows and becomes sharper, and at $n = 5$ and 6 it begins to split into a closely spaced doublet. By $n = 7$ and beyond, this doublet is clearly resolved and prominent. In the hydrogen-bonding region, the single peak at $n = 4$ (3180 cm^{-1}) evolves for the $n = 5$ spectrum into peaks at roughly 3195, 3357, and 3520 cm^{-1}. The $n = 6$ spectrum has bands at roughly the same positions as the 3357 and 3520 cm^{-1} features seen for $n = 5$, but the more strongly red-shifted feature for $n = 5$ at 3195 cm^{-1} has dropped noticeably in relative intensity. For $n = 7$ and larger clusters, this band is only present as part of a sloping background. Larger clusters have the hydrogen-bonding signal just in the region of 3400−3600 cm^{-1}.

These general observations are understandable in the context of a growing and more highly connected hydrogen-bonding network around the metal cation. It is easy to see why the symmetric stretch band recedes in importance relative to the asymmetric stretch. For a water molecule to contribute to the asymmetric stretch, it can have either just one or both OH groups freely vibrating, while a symmetric stretch requires that both hydrogens are unhindered. As the hydrogen-bonding network grows, fewer water molecules have both hydrogens free, and there are fewer oscillators that can contribute at the symmetric stretch frequency. A similar argument explains the spectra in the hydrogen-bonding region. We can recall from the discussion of Figure 6 that the most red-shifted bands here are those associated with "dangling" water molecules connected via only one hydrogen bond, while the less red-shifted bands are associated with more highly connected hydrogen-bonded species. As the network grows, there are more molecules that have higher connectivity, and the hydrogen-bonding resonances in the 3400−3600 cm^{-1} region become more likely.

Another interesting feature of the spectra in the $n = 4-10$ size range is the emergence of the doublet from the 3700 cm^{-1} asymmetric stretch band. This same kind of doublet behavior for this band has been described and discussed in our work[61] and that of others[55h−i,58f] on protonated water clusters. Because this resonance occurs near 3700 cm^{-1}, both of the doublet members must arise from molecules that have at least one free OH oscillator. However, as described in the previous work, the resonance of the free OH band can be affected by the secondary connectivity of the water molecules. In the discussion above for smaller clusters, this was noted to occur when there were metal-bound versus hydrogen-bonded water molecules present. Here, a similar effect can be seen for different kinds of hydrogen-bonding environments. Some water molecules are partially connected in the network, having one hydrogen involved as a donor to another water and one lone pair accepting a hydrogen bond from another water (i.e., an "AD" configuration). Other waters are more fully connected, donating one hydrogen and accepting two protons from two other waters (i.e., an "AAD" configuration). These "two-coordinate" and "three-coordinate" water molecules, respectively, feel slightly different inductive forces from their connectivity, and their free OH vibrations then have slightly different frequencies. As in the protonated water systems, the more highly connected AAD water molecules are assigned to have the resonance at the lower frequency and the two-coordinate AD species give rise to the higher frequency band. In the protonated water clusters,[55i,58f,61] the highly symmetric $H^+(H_2O)_{21}$ cluster, which is calculated to have a nearly icosahedral structure, was shown to have only the lower frequency band, while other clusters smaller or larger

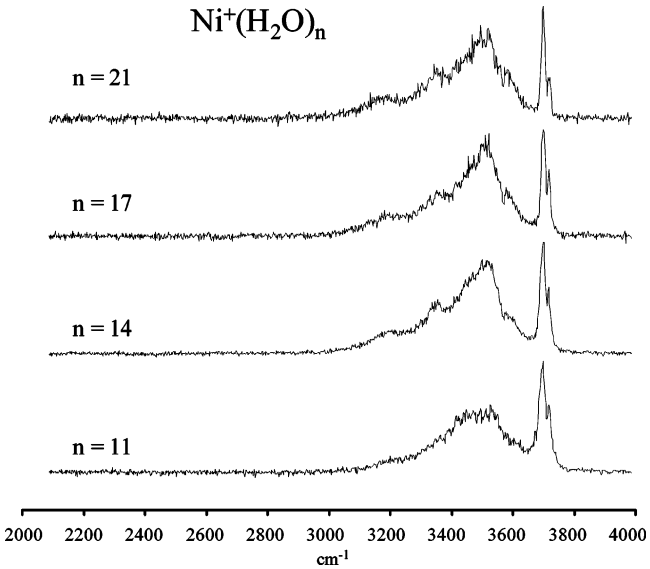

Figure 8. IR photodissociation spectra of the $Ni^+(H_2O)_n$ complexes for n = 11, 14, 17, and 21.

than this had both the AD and AAD bands. This same assignment seems reasonable to explain this doublet band in the $Ni^+(H_2O)_n$ complexes.

Figure 8 shows the spectra measured for selected clusters in the higher size range of $n = 11-21$. The other cluster sizes (not shown) in this same size range have spectra that are essentially the same as these in appearance. We have measured spectra over the full frequency range available (2050−4000 cm^{-1}) for all the clusters (except $n = 2$) up to $n = 25$. We have also measured the O−H stretch region for selected larger clusters ($n = 28$ and 30). The band positions derived from these spectra are presented in Table 3. The larger clusters in the $n = 11-21$ size range have an appearance similar to that of the smaller clusters, except that the hydrogen-bonding region of the spectrum has less structure on it and the intensity gradually peaks closer to 3500 cm^{-1}. As we mentioned above and discuss related to Figure 5, this is the region where hydrogen-bonding resonances occur when the network is more highly connected. It is therefore understandable that the intensity would shift toward this as the clusters become larger. All of these clusters also have the 3700 cm^{-1} doublet band.

It is natural to consider a comparison of spectra of clusters in the higher size range to those of other clusters containing water or those of bulk water systems. The infrared spectrum of water itself has been well-known for many years,[50−54] but there has been much recent interest in the IR spectroscopy of ice films prepared in different ways on different metal or oxide surfaces.[72−75] However, both the bulk liquid and ice spectra have more intense absorption in the hydrogen-bonding region and show little detail in the free OH region. Of more relevance to us, recent nonlinear laser spectroscopy methods have employed sum-frequency or difference-frequency spectroscopy for interfaces containing water.[76,77] Because these spectra probe only

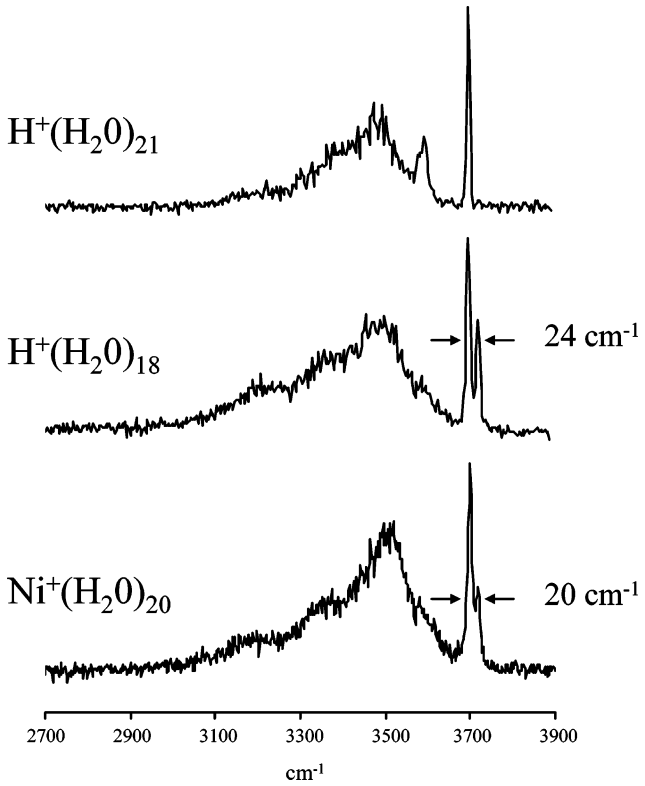

Figure 9. A comparison of the spectra measured for $H^+(H_2O)_{18}$ and $H^+(H_2O)_{21}$ with that measured for $Ni^+(H_2O)_{20}$.

the immediate vicinity of the water interface, they pick up resonances from both the free OH bands and hydrogen-bonded species. In fact, the present spectra have very nearly the same relative intensities in the hydrogen-bonding region versus the free OH region as these interfacial spectra, consistent with the fact that most of the molecules in our clusters are in fact residing at the water−vacuum interface. However, the free OH region is a broad single peak in the interfacial spectra; there is insufficient resolution to resolve the doublet structure that we see, or to decide if it is present at all in these interfacial spectra.

As noted above, we have recently been involved in similar studies on protonated water clusters in this same size range.[61] As shown in Figure 9, these protonated water clusters have IR spectra that are also very much like the ones that we are measuring here, with both a broad resonance in the hydrogen-bonding region peaking near 3500 cm^{-1} and a sharp structure near 3700 cm^{-1} attributed to the free OH resonances. As discussed in our earlier work, the protonated water spectra also have the same kind of doublet feature seen here near 3700 cm^{-1}, and it is assigned the same way that we do here to the presence of AD and AAD water molecules in the structure. In the case of the anomalous species $H^+(H_2O)_{21}$, we found that the 3700 cm^{-1} doublet collapsed to a single sharp peak at the AAD resonance, indicating a cluster with a highly symmetric structure with all water molecules in essentially the same environment. This was consistent with calculations for the $H^+(H_2O)_{21}$ cluster

(72) Mate, B.; Medialdea, A.; Moreno, M.; Escribano, R.; Herrero, V. J. *J. Phys. Chem. B* **2003**, *107*, 11098.
(73) Zelent, B.; Nucci, N. V.; Vanderkooi, J. M. *J. Phys. Chem. A* **2004**, *108*, 11141.
(74) Daschbach, J. L.; Dohnalek, Z.; Liu, S.-R.; Smith, R. S.; Kay, B. D. *J. Phys. Chem. B* **2005**, *109*, 10362.
(75) Hawkins, S.; Kumi, G.; Malyk, S.; Reisler, H.; Wittig, C. *Chem. Phys. Lett.* **2005**, *404*, 19.
(76) (a) Richmond, G. L. *Annu. Rev. Phys. Chem.* **2001**, *52*, 357. (b) Richmond, G. L. *Chem. Rev.* **2001**, *102*, 2693.
(77) Mucha, M.; Frigato, T.; Levering, L. M.; Allen, H. C.; Tobias, D. J.; Dang, L. X.; Jungwirth, P. *J. Phys. Chem. B* **2005**, *109*, 7617.
(78) Jiang, J.-C.; Wang, Y.-S.; Chang, H.-C.; Lin, S. H.; Lee, Y. T.; Niedner-Schatteburg, G.; Chang, H.-C. *J. Am. Chem. Soc.* **2000**, *122*, 1398.

which indicate that there are many closely related isomers having near-icosahedral structures, such as the clathrate structures found in nature.[61] Additionally, a somewhat sharp additional resonance was seen to emerge from the hydrogen-bonding region, centered at 3550 cm^{-1}. This was assigned to hydrogen-bonding species in five-membered rings on the basis of the previous conclusions of Chang and co-workers for the smaller protonated water clusters.[55f] Interestingly, the present $Ni^+(H_2O)_n$ clusters never have a single peak in the free OH region but rather always have the doublet structure here. Likewise, the spectra of the $Ni^+(H_2O)_n$ clusters do not ever have any resonance near 3550 cm^{-1} like that associated with five-membered rings in the protonated water species. We therefore conclude that the $Ni^+(H_2O)_n$ clusters do not have the same kind of high-symmetry structures in which all or nearly all molecules occupy the same positions in five-membered rings. This makes sense on the basis of the coordination of Ni^+ in these clusters. As we have already shown in Figures 5 and 6, Ni^+ prefers to have a coordination of three or four water molecules in the small clusters, and it is reasonable to assume that structures such as these form the core of the larger clusters. With such a coordination at the core of the cluster, it would be very difficult for hydrogen-bonding networks to form that result in the overall 5-fold symmetry found for the protonated water species. It is more likely that there are a number of related clusters with more varied isomeric structures. Essentially, the ensemble average of these structures may be more representative of amorphous water. If this logic is correct, then it would be very interesting to study water clustering around metal cations with different coordination numbers (e.g., five or six) where more symmetric hydrogen-bonding networks could form.

A final interesting aspect of these spectra is the value of the spacing between the asymmetric stretch doublet at 3700 cm^{-1}. The spacing between these doublet bands is not constant for different cluster sizes. As can be seen from the band position entries in Table 3, the spacing is approximately 24−25 cm^{-1} when it first emerges in the smaller clusters, but this decreases gradually, becoming more like 20 cm^{-1} in the largest clusters. Such a decrease in this spacing is understandable, because it represents the difference in the environment of AD versus AAD water molecules, and this difference should become smaller as molecules are located on the surface of the cluster away from the metal cation. Early models of metal cation solvation describe the different spheres of coordination around a central metal cation and how the solvent molecules experience a polarization or charge inductive effect in their electronic structure, either through direct contact with the metal or through the hydrogen-bonding network.[2] This polarization diminishes as water molecules are in the second or subsequent solvation spheres. The solvation spheres in our clusters will vary depending on the exact structures that these species have. However, if we assume that the immediate coordination around the cation is three or four molecules, then the larger clusters that we study ($n = 20-25$) must have mostly second-sphere molecules, and they probably have some water twice-removed from the metal in a partially formed third sphere. It is understandable then that the doublet spacing of the asymmetric stretch, which is one manifestation of the overall inductive interactions in these clusters, should become smaller as the cluster size grows.

Another interesting aspect of the 3700 cm^{-1} doublet feature is its behavior in these $Ni^+(H_2O)_n$ clusters compared to the corresponding protonated water clusters.[61] This comparison is shown in Figure 9. As indicated in these representative spectra, the doublet spacing is not the same for the $Ni^+(H_2O)_n$ versus $H^+(H_2O)_n$ clusters. Although there are small variations with size, the doublet spacings in the protonated water clusters in the size range near $n = 20$ are all in the neighborhood of 24 cm^{-1}, while those for $Ni^+(H_2O)_n$ in this same size range are more like 20 cm^{-1}. This is a small difference, but it is within our experimental resolution. It implies that the inductive forces caused by the cation in these clusters can be felt to different degrees when the cation is a proton versus Ni^+. If we could study much larger clusters, there would presumably be a size for which the identity of the cation would no longer be apparent and the AD−AAD doublet spacing would converge to an as yet unmeasured "bulk" value.

Conclusion

We have reported a study of the solvation processes represented by $Ni^+(H_2O)_n$ clusters. Size-selected infrared photodissociation spectroscopy, supplemented by density functional theory calculations, monitors the kind of infrared oscillators present in these systems and how they evolve with cluster size. In the smallest clusters, water molecules are coordinated directly to the metal cation and the free OH stretches are shifted to lower frequencies because of the resulting polarization of bonding molecular orbitals on water. Beginning at the cluster size of $n = 4$, there is evidence for hydrogen bonding, and this grows and becomes more important in the larger clusters. Because of the formation of the hydrogen-bonding network, the symmetric stretching mode seen in the free OH region loses intensity in the cluster size range of $n = 6-8$. By $n = 10$, the asymmetric stretch resonance becomes the signature of those water molecules with one free OH remaining. This free OH resonance splits into a doublet caused by the different inductive forces present for two-coordinate versus three-coordinate water molecules. In the largest clusters studied, there is a broad region of hydrogen-bonding signal and the closely spaced free OH doublet. These spectra have strong similarities to the IR spectra measured previously for protonated water clusters or for water molecules at the liquid−air interface. A comparison of $Ni^+(H_2O)_n$ and $H^+(H_2O)_n$ molecules in the size range near $n = 20$ shows that the nickel systems do not attain high-symmetry structures like those reported for protonated water clusters. This is presumably because the coordination of singly charged Ni^+ at the core of these clusters is three or four water molecules, and this does not provide a good template for 5-fold symmetric growth like that seen for protonated water. Additionally, the doublet spacing at the free OH resonance is not the same in the nickel cation versus protonated water clusters. The induction forces running through these clusters are still strong enough in this size region so that the cation identity makes a difference.

This is the most extensive spectroscopic study yet on the solvation processes in metal cation−water clusters. Future studies are warranted on other metals with different coordination numbers and different charge states to test the ideas suggested here. Likewise, more sophisticated theory is needed to test the various isomeric structures that are possible in the larger clusters

and to investigate the inductive forces running though these hydrogen-bonding networks.

Acknowledgment. We appreciate the support of this work by the U.S. Department of Energy through Grant DE-FG02-96ER14658.

Supporting Information Available: Full citation for ref 63 and full results of our density functional theory calculations on the various $Ni^+(H_2O)_n$ complexes ($n = 1-5$) and their corresponding argon-tagged analogues (these data includes structures, energetics, and vibrational frequencies for the different isomeric structures at each cluster size). This material is available free of charge via the Internet at http://pubs.acs.org.

JA0542587